Mine Water Environ (2011) 30:274–283
DOI 10.1007/s10230-011-0158-0

TECHNICAL ARTICLE

Analysis of Groundwater Inrush Conditions and Critical Inspection Parameters at the Baixiangshan Iron Mine, China

He Keqiang · Yu Wancheng · Jiang Wenfu

Received: 30 June 2010 / Accepted: 15 July 2011 / Published online: 31 July 2011

Abstract The Baixiangshan Iron Mine is a large, complex deposit. The mine is endangered by several groundwater inrush factors: multiple aquifers, high water pressure, transmissive faults, and minor hidden faults, joints, and fissures. Through a systematic hydrogeological investigation, locations where the major roadway intersected with faults in the aquifers were identified. Critical inspection parameters to predict the potential of groundwater inrush were then calculated for the intersections between the major roadways and the transmissive faults. Finally, control measures are proposed that incorporate the high groundwater pressure and the high dip angle faults. The results of this research can be applied during development of the Baixiangshan Iron Mine.

Keywords Baixiangshan iron mine · China · Control measures · Critical inspection parameter · Groundwater inrush · Hydrogeological conditions

Introduction

Research has been conducted on groundwater inrushes in mines since at least the 1950s. Field observations led to the use of an impermeability coefficient as a potential inrush indicator and consideration of impermeable strata, along with an explanation of circumstances leading to disruption of an impermeable mine floor, based on an energy balance perspective (Dyskin and Germanovich 1995; Jiefan et al. 1993). From the 1970s until the 1990s, researchers in rock mechanics in many countries examined the mechanism of floor damage in their study of mine prop stability (Kulatilak et al. 1993). Åkesson (1983) described a hydrogeological and geotechnical study of rock mass at an experimental nickel mine at Lappvattnet, Sweden. That study showed that there was a strong need to modify grouting methods to suit rock conditions in order to control groundwater incursions. The need for a detailed geotechnical investigation prior to the planning and design stage of a project was also discussed (Åkesson 1983). Bouw and Morton (1987) presented a procedure to rationally assess the potential of inflows based on the interactive operation of two computer models: an inflow model and a groundwater finite element model. Both were calibrated using information obtained from aquifer monitoring.

C. F. Santos and Z. T. Bieniawski analyzed the bearing capacity of the floor in light of the improved Hoek–Brown rock mass strength criteria and the concept of a point of critical energy release (Geir 1992; Paul et al. 1993). Analysis of the various system components indicated that several key factors would have to be modified to consider the effects of mining, subsidence, and groundwater rebound. According to the statistical data in Hungary, 75–80% of groundwater inrushes occurred along faults, 16–21% in fractured zones, and only 4% were not related to geologic structures (Zhixiang 1999).

Chinese researchers have also contributed to this research. After Qian Minggao put forward his key strata theory, Shi and Qu (2000) published their mine pressure theory, which centered on strata movement. Liu Tianquan and Zhang Jincai proposed their plate model, zero position

H. Keqiang (✉) · J. Wenfu
Department of Civil Engineering, Qingdao Technological University, Qingdao, Shandong 266033, People's Republic China
e-mail: keqianghe@sina.com

Y. Wancheng
Experiment Base of Professional Education of Qingdao, Qingdao 26611, People's Republic China

disruption, and in situ rupture hypotheses. Other researchers investigated the mechanism of groundwater inrush in mines and related risk assessment by means of mathematical statistics, hydromechanics and rock mechanics, computer simulation recognition, GIS, and composite computation of multi-source data.

Research on the prevention of water-related disasters and the detection of karst features and fractures has also been going on worldwide. Here, we report on the systematic investigation of hydrogeological conditions in the Baixiangshan iron mine, in China. We analyzed where the major mine roadway intersected faults in the aquifers and determined potential inrush channels and groundwater inrush determining factors. Critical inspection parameters to prevent a groundwater inrush were calculated for the intersections between the major roadways and the transmissive faults of the mine, and potential control measures are proposed that incorporate the high groundwater pressure and the high dip angle faults.

Site Characteristics and Hydrogeological Conditions

Site Characteristics

The Baixiangshan Mine is 12 km from Dangtu County, southeast of AnHui Province, and 2.5 km from the Gushan Mine (of the Magang Group) (Fig. 1). The area of the ore body is about 1.4 km^2, with its main section buried at depths of −200 m to about −600 m. The current estimate of the geological reserves is 150 million tons. The designed annual yield is two million tonnes (t) of iron, of which magnetite output will account for 90.2%, with an average grade of 36.4%. The mine is designed to develop three main horizontal major roadways at a depth of −390, −450, and −495 m respectively. The prospecting data indicates that the mine will be water-rich and thus difficult to exploit.

Construction of the mine infrastructure and the safety of the miners have already been jeopardized by mine water inrush events. On August 26th, 2006, after tunneling had proceeded for 84.3 m at a level of −470 m, a huge groundwater inrush (approximately 260 L/s) occurred during the process of blasting and clean-up, flooding the air shaft. Moreover, on April 6th, 2008, as the auxiliary shaft was being developed at a level of −80 m, another inrush occurred; the flow reached approximately 11.1 L/s. The hydrogeological conditions of the mine and documented instances of major water incursion show that groundwater represents a major hazard. The groundwater appears to be principally associated with prominent faults, minor hidden faults, and joints; these are possibly connected by poorly sealed drill holes. To prevent or minimize future water inrush events during roadway excavation and mining,

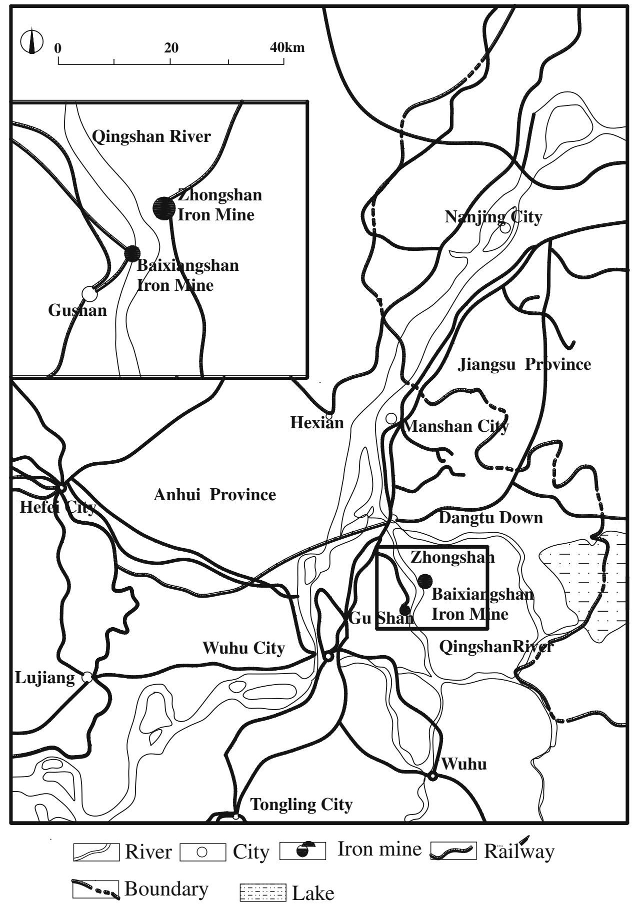

Fig. 1 Regional location of the Baixiangshan Iron Mine in China

additional clarification of the hydrogeological conditions and geological hazards was crucially needed. We started by compiling and examining all of the existing drilling and hydrogeological data for the mine area, used it to draft the profile of the east and west lanes of the major horizontal roadway at the −495 m level, and then determined where the roadway would intersect the faults and the aquifer.

Hydrogeological Conditions

The Qingshan River overlies the southern portion of the mine and flows from North to South. The river is about 100 m wide, and flows on a flood plain that is 200–300 m wide. There are canals on both sides of the river. Approximately 20% of the region's precipitation reaches the Qingshan River and its tributaries.

Initial identification of the hydrogeological boundary conditions showed that the unit is largely impermeable in the northeast and in the southwest due to diorite strata. The hydraulic conductivity, in general, varies from 0.01 to 8.25×10^{-5} m/d (Table 1). The groundwater dynamic monitoring curves of these strata during pumping tests are shown in Figs. 2 and 3. The shale zone of the Huangmaqing

Table 1 The hydrogeological parameters of the main aquifers and aquicludes in Baixiangshan iron mine area

Aquifers and aquicludes	Specific capacity, q (L/s·m)	Hydraulic Conductivity k ($\times 10^{-5}$ m d^{-1})	Static water level elevation (m)	Effective fissure ratio (%)	Thickness and elevation (m)
The pore aquifers and aquicludes of Quaternary system					
1. The low permeability aquifer between silty fine sand and loam of the Holocene of Quaternary system: Q_4^{4al}---II_4	0.01	0.14	–	–	0.00–26.34, The average is 12.37 in the fluvial plain south and west of orefield; The elevation of bottom is –19.78–2.60
2. The low permeability aquifer between silty fine sand and of loam the Holocene of Quaternary system: Q_4^{3al}---II_3	0.13–0.15	1.05–1.43	6.10	–	0.47–31.00, The average is 13.50. The bottom contacts with aquiclude of loam.
3. The aquiclude of loam of the Holocene of Quaternary system: Q_4^{2al}	–	–	–	–	1.25–23.74. The average is 12.07.
4. The high permeability aquifer of sandy gravel stratum of the Holocene of Quaternary system: Q_4^{1al}---I_1	0.81–17.35	6.08–52.80	3.19–3.63	–	1.86–15.40, The average is 8.85; The elevation of bottom is −39.56 to −48.39.
5. The low permeability aquifer of loam mingled with gravel of the Pleistocene of Quaternary system: Q_3^{al}---II_4	0.01	0.11–0.28	4.25–1.57	–	0.00–21.39, The averagely is 9.31; The elevation of bottom is 30.88–32.77
The fissure aquifers and aquicludes of bedrock					
1. The low permeability aquifer of upper volcanite of lower Cretaceous system: K_1---I_3	0.05	0.10	3.51	–	20.00–370.00
2. The low permeability aquifer of feldspar quartz sandstone of Xiangshan group of the middle and lower Jurassic system: J_{1-2}---I_3	0.03	0.01	The northeast 16.68–45.00; The west 3.60	–	The maximum is 287.65, The average is 150.00
3. Aquifer of shale of Huangmaq ing Group of Upper Triassic system					
The medium permeability aquifers of Purple shale of Huangmaqing group: T_3h^2---I_2					
Most area except the epotential for recharge	0.14	0.16	4.35–7.64	0.00–3.55	17.39–426.11, The average is 125.34
The northern portion of the mine	0.49–0.55	1.34–2.55	–	–	
The high permeability aquifers of mottled fine sandstonof Huangmaqing groupe: T_3h---I_1					

Table 1 continued

Aquifers and aquicludes	Specific capacity, q (L/s·m)	Hydraulic Conductivity k ($\times 10^{-5}$ m d^{-1})	Static water level elevation (m)	Effective fissure ratio (%)	Thickness and elevation (m)
Anticline axis	2.46–8.20	1.72–12.60	3.00–4.00	0.60–2.14	16.96–263.51. The average is 112.42. The elevation of top is −23.97 to −474.96. The average is −112. 27 The elevation of bottom is −55.12 to −536.60
West wing	0.30–0.94	0.62–2.45			
East wingTransmissivity KM = 17.36 × 10^{-5} m^2 s^{-1}					
The high permeability aquifer in the south of F3	3.35	3.12	−1.12	–	About 140.00. The elevation is below −354.00.
Northwest high permeability aquifer	2.51	8.94	9.14	–	About 100.00. The elevation is below −389.45.
The low permeability aquifer of hornfelsized sandy shale of Huangmaqing groupe: T_3h^1---I_3	0.01–0.03	0.01–0.07	–	0.00–0.63	0.00–312.02. The average is 93.48.
4. The aquifers of ore bearing layer					
The medium permeability aquifer in the south: Fe---I_2 with Kaolinization, Karbonationization and silicification))	0.10–0.66	0.09–1.11	–	0.00–0.98. The average is 0.22.	0.81–529.56. The average is 143.29. It has hydrological connection with upper aquifers. So they became an unified aquifer.
Low permeability aquifer in the north Fe---I_3 (with Kaolinization and epidotization)	0.01–0.03	0.02–0.05	–		
5. The low permeability aquifer of rock:					
Diorite of bottom wall of strata containing minerals	0.01	0.01	–	0.00–0.43. The average is 0.15	–
Wanjiashan diorite in the east of Baixiangshan	0.03	–	24.10–100.51	–	–

The specific capacity, Hydraulic Conductivity, Static water level elevation and effective fissure ratio are determined by dewatering test, pumping test, drilling test of group of holes and pumping test in the Baixiangshan mining area respectively

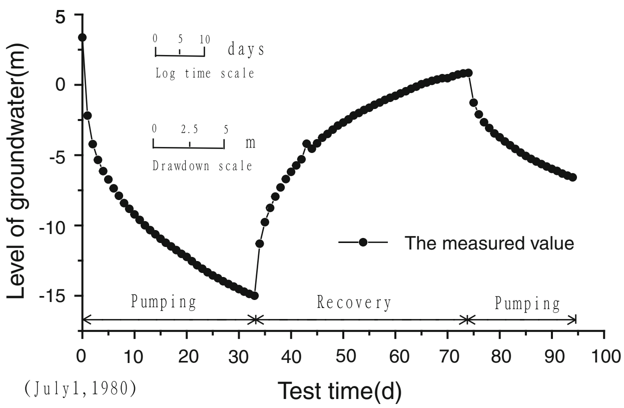

Fig. 2 A groundwater dynamic monitoring curve of a saturated moderately permeability sandstone stratum

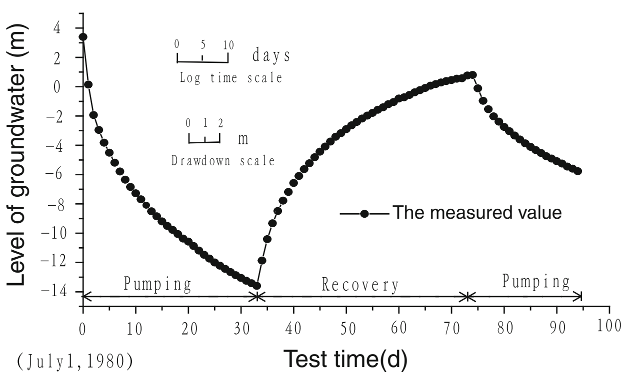

Fig. 3 The groundwater dynamic monitoring curve of a saturated highly permeable sandstone aquifer

group, which is only moderately permeable, is missing between exploration line 2 in the north and exploration line 7 in the south. As a result, an area of 2.09×10^5 m^2 in the southern part of the mine offers greatly enhanced potential for recharge, and transmits a high amount of infiltration through a siltstone aquifer of the Huangmaqing group of the Upper Triassic.

There are eleven major faults (F1–F11) distributed in the area, mainly in the central and southern part of the mine, with different intersections between the major roadway and connected roadways at three different levels of infrastructure: −390, −450, and −495 m, respectively. These faults are filled with breccias and fine-grained syenite or diabase. Alteration to sericites and chlorites has caused the faults to have high water transmissibility and permeability.

In addition, a large number of unsealed or poorly sealed drill holes have been left from geological exploration (Christian 2004; Pang 2007; Zhang and Tan 2005). These drill holes penetrate each aquifer and the impermeable strata, changing the original distribution structures and relationships. Some are close enough to the river and its tributaries that they probably serve as drainage channels during storm events (Zhan 1978). When blasting is conducted nearby, inappropriately sealed drill holes are made more permeable due to vibration (Yan and Li 2007). All of these factors make the complicated hydrogeological conditions of the Mine even more complex.

Groundwater Inrush Data

As previously mentioned, on August 26, 2006, a groundwater inrush event (approximately 260 L/s) occurred at the working face, flooding the air shaft. The event was caused by a rock burst through a fragmented zone in the fault, F4, triggered by tunneling at the working face.

The geological records of the air shaft show that the strata are mainly diorite, and that there are more than 12 exposed minor fault zones, with widths ranging from 0.1 to 0.8 m. The fault zones generally contain broken and fractured rock. There are 5 faults that reach upwards to an elevation of at least −130.2 m and 7 faults that extend from an elevation of −320 m to at least the bottom of the mine. At the same time, there are many tension or compression-shear joints in the shaft; these are filled with calcite or chlorite. In some joints, there are clear signs of groundwater infiltration. During construction, it was found that there are a group of tension joints with a dip of 78°–82° at elevations of −111.0 to −120.1 m, partially filled with calcite, through which water flows into the mine (Fig. 4). In addition, some rocks show signs of sidewall scaling.

When the first stage of grouting through the tunnel walls was finished, the amount of groundwater inflow decreased from 3.5 to 9.3 L/s (at an elevation of −154.2 m), but flow increased to approximately 6.9 L/s at the −116.4 m elevation. A second stage of grouting through the tunnel walls further reduced the amount of groundwater inflow to approximately 1.1 L/s (at an elevation of −170.2 m). After this, as the depth of construction increased, ground water inflow stabilized at a range of 1.1–3.5 L/s.

Minor faults and joints exist in both the deep and shallow rock masses; shallow level strata are fragmented and kaolinized, and contain faults and joints that transmit large

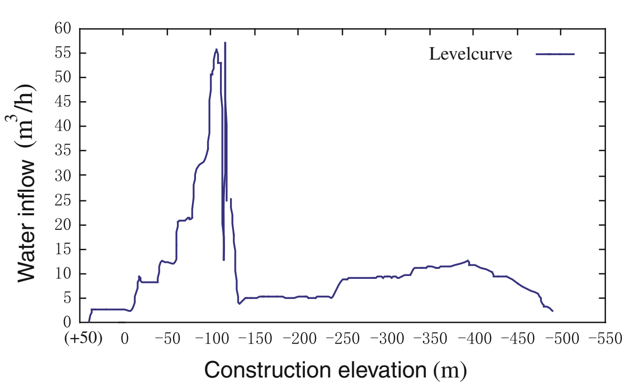

Fig. 4 A diagram of water inflow during construction of the air shaft

amounts of water. The deeper diorites are hard and relatively unweathered; therefore, although they contain faults and joints are hydraulic, only a small amount of water flows from them into the mine.

From the hydrogeological conditions of the deposit and the groundwater inrush events that have already taken place, it can be concluded that the major faults, minor hidden faults, and fissure joints, and poorly sealed drill holes together represent potential main water disasters to the infrastructure, construction, and exploitation of the Baixiangshan iron mine.

Intersections of Roadways and Major Faults

Six major faults (F2, F3, F4, F5, F6, and F7) intersect the deposit. Major faults F2 and F3 preceded mineralization. The western lane of the major −495 m roadway intersects the southern tip of faults F3 and F5 (as shown in Fig. 5) while the parallel eastern lane, 1080 m away, intersects the central portion of F4 and F5 (as shown in Figs. 6 and 7).

F3 is normal displacement fault with a width of 50–100 m, a vertical displacement of 100 m, and a horizontal displacement of 50 m. This fault was filled with diorite rock, accompanied by sand, shale and breccia, much of which is cemented by iron and siliceous materials. Fissures are developed in the upper part of these faults and are filled with calcite and kaolinite, with an effective fissure rate of 1.4%. The effective fissure ratio decreases gradually with greater depth. Fault F3, which has a specific capacity (q) of 0.219–0.368 L/m s and a permeability coefficient (k) of 0.21–0.59 $\times$ 10^{-5} m/d, is the permeable border at the southern end of the mine.

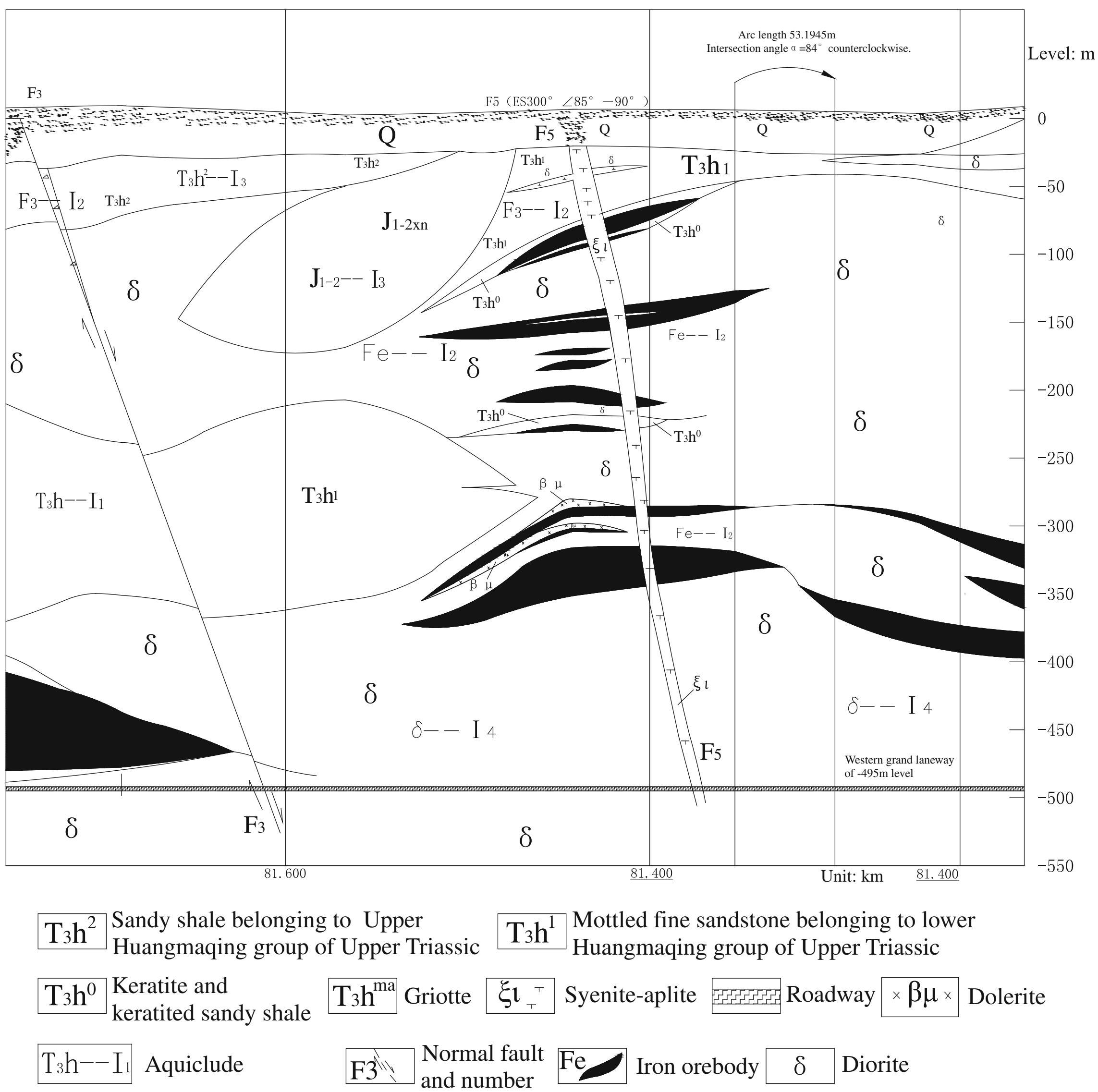

Fig. 5 Profile of faults F3 and F5 where they intersect the western lane of the mine's major roadway

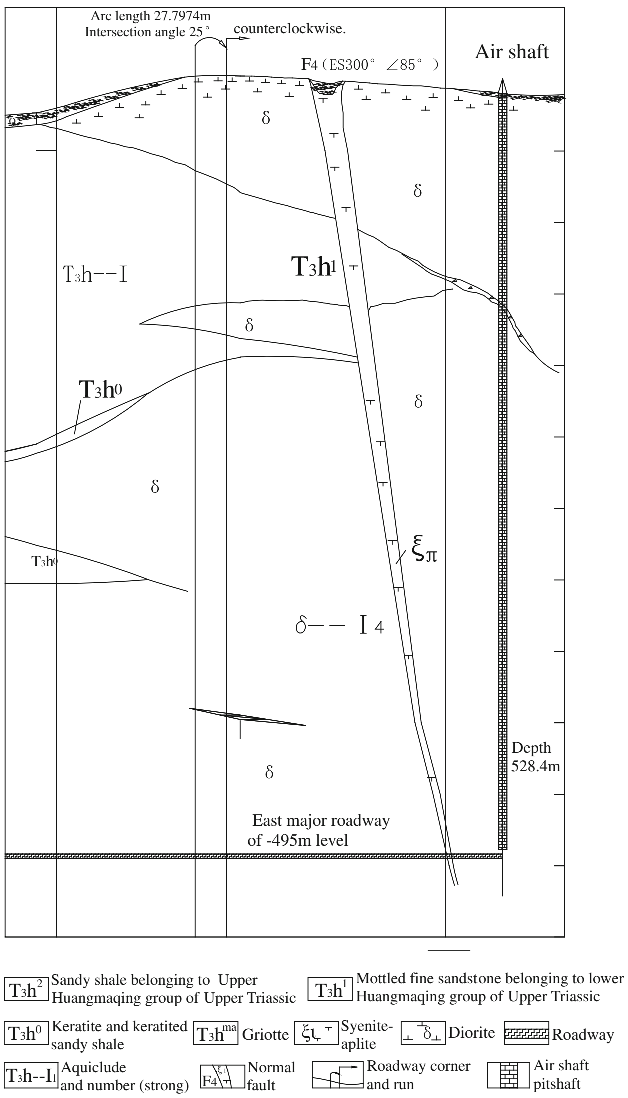

Fig. 6 Profile of fault F4 where it intersects the eastern lane of the mine's major roadway

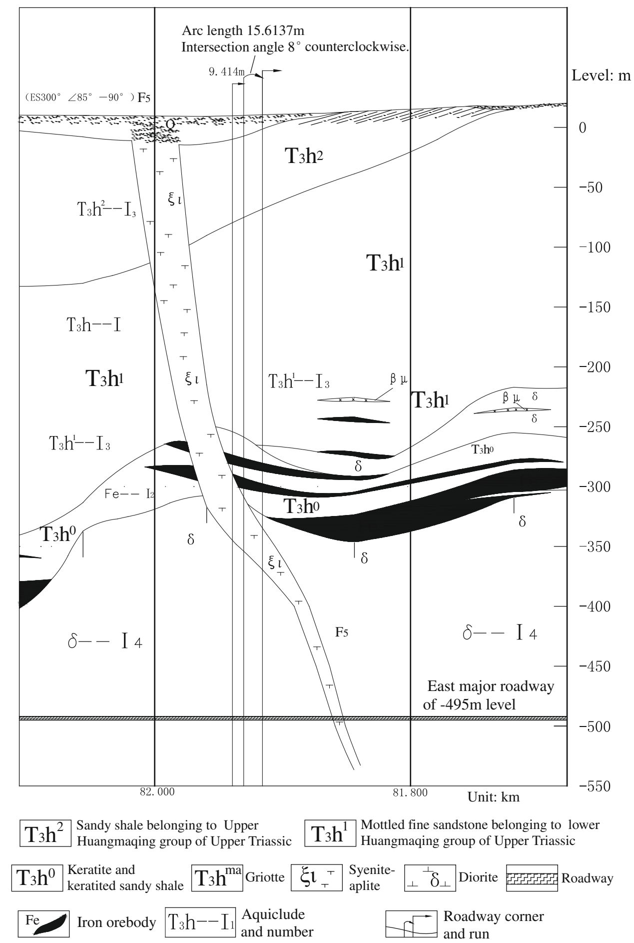

Fig. 7 Profile of fault F5 where it intersects the eastern lane of the mine's major roadway

The overall strike of F5 is approximate NE 30°, with a tendency towards the SE and a dip of 75°–85°. F5 is a tension fault and is filled with a red, fine-grained syenite-aplite. Also, this fault curves and pinches out in spots, generally ranging in width from 5 to 10 m, with one expanded portion of 15–20 m. The eastern portion of the fault shows a large number of slickensides and extends downwards, where the rocks on both sides have been crushed.

F4 is a normal fault with a strike of NE 30° and a dip of more than 85°. It is filled with orthophyre, with a variable width of 5–10 m. The fault contains angular rock fragments, 1–5 cm in size. In some locations, an off-white and kaolinized fault gouge is visible, together with broken rocks on both sides of the fault, which extends about half a kilometer to Baozi Mountain in the northwest and at least 87.5 m to the southeast of the mine. At a level of 7–8 m to the east of the fault, a small Quaternary-age fault is an additional source of water. It extends over 400 m, and is around 3 m in width at a depth of −500 m.

Groundwater Inrush Risks and Critical Inspection Parameters

Groundwater inrush events that occur at the intersections of major roadways and faults are affected by: the permeability and degree of cementation of the faults; the height of the transmissibility fissure zone caused by the unloading of wall rock during tunneling (Chen et al. 2006; Ni and Qian 1996); the distance between the faults and aquifers; the amount of water in the aquifers (Tan 1999); and the water pressure in the broken zone along the fault (Jiang et al. 2005; Li 2006).

From top to bottom, the upper part of F3 (with an average thickness of about 50 m), intersects mineralized granitic strata (average thickness about 180 m), which is moderately permeable, the highly permeable fine-grained

Huangmaqing sandstone aquifer (average thickness about 120 m), and a stratum of diorite (average thickness about 60 m) (Fig. 5). The thickness of the strata is not significantly affected by their intersection and displacement by F3. The upper part of F5 (average thickness about 60 m), cuts through the same granitic strata, which is more than 300 m thick at this location, and the diorite, which is more than 100 m thick (Fig. 5).

F4 intersects the eastern lane of the mine's major roadway about 110 m from where the air shaft intersects the roadway (and about 40 m the air shaft). As shown in Fig. 6, most of F4 is in the diorite body, with only its upper portion (at about −45 to −110 m) cutting through the sandstone aquifer. In contrast, the part of fault F5 that intersects the eastern lane of the major roadway cuts through about 150 m (at about −100 to −260 m) of this aquifer at the axis of an anticline. Therefore, the groundwater inrush risk of F5 is greater than that of F4.

In addition, F2, which predates mineralization, is located west of the major roadway. It is a large scale normal tensional fault with a dip of about 70°–80°. The shortest distance between F2 and the western lane of the major roadway is approximately 50 m; between F2 and the roadway is the mineralized sandy shale, which is moderately permeable. F2 is mainly filled with fragments of sandy shale, diorite, syenite-aplite, diabase, and aplite and is cemented by diorite, skarn, and iron. The cementation in the upper part is poorer than that in the lower part. The effective fissure ratio is 1.13%. The specific capacity is 0.314–0.531 L/m s, while the hydraulic conductivity is $1.17–1.75 \times 10^{-5}$ m/d.

F2 connects the low permeability sandstone of the western side of Xiangshan Group with the Quaternary porous aquifer. Therefore, to reduce the groundwater inrush risk, F2 and the sandy shale strata that lies near the roadway should be grouted (Mostkov 1998; Paul 2004; Wang et al. 2007).

Grouting of faults should proceed in four steps:

1. When the fault or an aquifer will intersect the roadway or mine workings, the structural conditions and the hydrological conditions should be investigated through advance borehole drilling and geophysical prospecting; based on the results, a pre-grouting plan should be developed, considering the water pressure, fracture status, slit width, etc.
2. Before large-scale grouting, an on-site preliminary grouting test should be performed to obtain parameters such as the final pressure for grouting, the grouting material (grouting proportions, etc.), the filling capacity of the grout, and to confirm that the grouting procedure selected is appropriate.
3. Dewatering tests and rock sample inspections through drilled inspection holes should be used to evaluate the result of the grouting; grouting should be repeated, if necessary.
4. Excavation can then be continued, with post-grouting and timely sealing of the roadway walls performed at local fracture zones and small water entry points.

These procedures should, at least in part, shut off the water supply from the aquifers above and to the west of the roadway, thereby reducing the quantity of discharged water and providing long-term roadway stability (Qiu 2002).

Based on the rock conditions and from what occurred during construction of the air shaft, there are other unknown sub-faults, in addition to the major faults discussed above, that could also contribute to groundwater inrush. Especially along the axis of the local anticline, tenso-shear joints have the ability to transmit water towards the mine. Therefore, beneath this area, the degree of advanced detection should be increased during construction and exploitation.

Given the transmissive features of the major faults, and the fact some of these faults directly intersect the roadways, making such locations highly susceptible to groundwater inrush, it makes technical sense to treat these locations with extra caution. A detailed and quantitative detection plan for such high potential groundwater inrush locations should be worked out to better define the water abundance and transmissibility of these intersections, before sealing is implemented.

1. The roadway is most stable when the angle of intersection between the fault and the roadway happens to be 90°. Therefore, where possible, roadways should be designed to intercept faults perpendicularly. When this is impossible, the greatest possible angle should be aimed for to maximize the stability of the roadway and its capacity against groundwater inrush.
2. When the major roadway and the faults are parallel or nearly so, it's best to have the roadway located in the foot wall of the fault. If part of the roadway has to be located in the top wall, it should be as small as possible.
3. In general, faults that contain water are more dangerous at deeper depths; advanced testing should consider this aspect and carefully measure water pressure in transmissive faults at various mining elevations.

The required width of impermeable rock columns can be obtained via the formula in the Code for Mining Hydrogeology (State Bureau of Coal Industry of People's Republic of China 1984).

$$S = 0.5AL\sqrt{\frac{3P}{K_p}} \tag{1}$$

Where: A = a safety factor of 2–5; L = breadth of the roadway or mining height (maximum)—the mine's

Table 2 Critical inspecting distances of ground-water at intersections between level roadways at −390, −450, and −495 m and faults F4, F5, and F6

Roadway elevation	Intersections	Safety factor value	Faults	Occurrence of fault	Included angle between fault and roadway plane	Hydrostatic pressure (Mpa)	Critical inspecting distances to the headon fault (m)
−390 m	390-1	5	F4	SE300°/∠85°	84°	3.9	41.9
	390-2	5	F5	SE300°/∠85°–90°	82°	3.9	45.2
	390-3	5	F5	SE300°/∠85°–90°	80°	3.9	45.5
	390-4	5	F5	SE300°/∠85°–90°	29°	3.9	92.5
	390-5	5	F5	SE300°/∠85°–90°	81°	3.9	45.4
	390-6	5	F5	SE300°/∠85°–90°	49°	3.9	60.1
−450 m	450-1	5	F6	SE140°/∠75°–85°	50°	4.5	59.6
	450-2	5	F6	SE140°/∠75°–85°	31°	4.5	88.7
	450-3	5	F5	SE300°/∠85°–90°	44°	4.5	69.9
−495 m	495-1	5	F4	SE300°/∠85°	81°	4.95	47.5
	495-2	5	F5	SE300°/∠85°–90°	53°	4.95	63.2
	495-3	5	F5	SE300°/∠85°–90°	58°	4.95	59.6
	495-4	5	F5	SE300°/∠85°–90°	46°	4.95	70.2

roadway is 3.8 m high; $P =$ hydrostatic pressure; and $K_p =$ tensile strength of the impermeable stratum.

The diorite, out of which the major roadway is dug, has a dry-condition compressive strength of 22.12—85 Mpa, with an average of 50.55 Mpa, ranking it among the lowest of all grade diorites. This poses a problem for both groundwater inrush prevention and the stability of the surrounding rocks. According to the rock mechanics section in the Handbook of Engineering Geology (4th Edition), the ratio between the tensile strength of diorite and its compressive strength is approximately 0.028. So, the actual measured value for the tensile strength of diorite (K_p), roughly 1.42 Mpa, can be obtained in terms of the compressive strength of diorite. Similarly, minimum compressive strength value obtained for the faults determine the corresponding tensile strength, which is approximately 0.62 Mpa.

After the dip angle of the faults and the included angles between the faults (F4, F5, and F6) and the various roadways (at −390, −450, and −495 m) were considered, Eq. 1 and the mine's hydrogeological conditions were used to calculate safe distances from the faults from which to conduct critical inspection parameters for investigations to avoid a possibly catastrophic inrush (Table 2).

Conclusions

1. The hydrogeological conditions of the Baixiangshan Iron Mine are complex. Part of the mine lies beneath surface water, and there is the risk of groundwater inrush through major faults, minor hidden faults, and joints. Poorly sealed hydraulic drill holes connect all of these. Groundwater inrush events endanger the infrastructure construction, mine exploration, and production.
2. Given the construction process in the mine's auxiliary shaft, and the way that the relatively impermeable diorite strata are distributed, the auxiliary shaft would appear to be an excellent venue for further advance exploration of major roadways. Major faults, minor faults, and tension and compression-shear joints are the main channels of groundwater inrush in the diorite. However, groundwater inrush events that have already occurred show that there are many potential water conduits at the Baixiangshan Mine, compared to other mining areas.
3. As shown by the intersections between major faults and roadway at the Baixiangshan Mine at the −495 m level, there are difficulties in predicting where and the amount of water that will enter the mine. F5 intersects the saturated sandstone stratum at a location where it has an average thickness of 150 m, near the axis of a local anticline. Water exploration and control should be focused on the associated jointing between the eastern portion of the major roadway and F5.
4. Critical inspection distances for advance water detection were calculated and the basic design principles for the intersections between the major roadways and the transmissive faults were proposed, based on eq. (1) and the mine's hydrogeological conditions.
5. Dewatering facilities should be established as soon as possible to enable the mine to better respond to a major water inrush. In addition, a dynamic groundwater monitoring drill-hole network should be designed and

developed for this mine. This network should be used to record the daily volume of influent groundwater, and to assess the influent flow during exploration to establish a statistical baseline for water inrush control and treatment.

6. The investigation and assessment methods for groundwater inrush risk proposed in this paper should be helpful in controlling and minimizing groundwater inrush hazards of other mines with similarly complicated hydrogeological conditions.

Acknowledgments The research discussed in this article was sponsored by the Open Research Foundation of Water Resources and Hydropower Research of China (IWHRKF 2010119) and the National Natural Science Foundation of China (projects 40672182 and 40872184). The authors express great gratitude to the technicians from Gushan Mine Industry Company of Ma Steel Trade Group, who offered great support and valuable information, including Wang Wenxiao, Deng Peidi, Sun Maogui, and Pan Baozheng. The authors also thank our hard working technicians, including Bai Jianye, Li Xiangran, and Li Xing.

References

Åkesson JA (1983) A study of geohydrological and rock engineering environment at Lappvattnet experimental mine. Mine Water Environ 2(3):25–38

Bouw PC, Morton KL (1987) Calculation of mine water inflow using interactively a groundwater model and an inflow model. Mine Water Environ 6(4):31–50

Chen R, Bai H, Feng M (2006) Determination of the height of water flowing fractured zone in overburden strata above fully-mechanized top-coal caving face. J Min Safety Eng 23(2):220–223

Dyskin AV, Germanovich LN (1995) A model of fault propagation in rocks under compression. Rock Mech 54(5):55–62

Geir J (1992) Discrete fracture modeling of in situ hydrologic and tracer experiments. In: Proceedings of International Conference on Fractured and Jointed Rock Masses, Lake Moe CA, USA 1(1):324–328

Huang J, Wang Z, Zhao Y (1993) The development of rock fracture micro fracturing to Main Fracture Formation. Rock Mech 30(7):925–928

Jiang YJ, Zhu D, Li, Qi (2005) The analysis of hole spraying during shed-pipe grouting passing through faults. Gr Pres Strata Contr 22(3):3–5, 8

Kulatilak P, Wang HS, Stephansson S (1993) Effect of finite size joints on the deformability of jointed rock in three dimensions. Int J Rock Mech Min 30(5):479–501

Li M (2006) A study of the mechanism of groundwater inrush and prevention measurements of the bauxite aluminium ore in Jiagou, Henan. Hydrogeol Eng Geol 33(5):85–89, 94

Mostkov VM (1998) Investigations of underground water-development works. Power Technol Eng 33:480–487

Ni L, Qian M (1996) Mechanism of groundwater inrush through fault. J China Coal Soc 21(2):119–123

Paul F, Hudak HA, Loaiciga E, Schoolmaster A (1993) Application of geographic information system to groundwater monitoring network design. Water Resour B 29(3):383–390

Shi Q, Qu Y (2000) Method determine water inrush from a fault in floor. Ground Press Strata Control 2000(2):33–35

State Bureau of Coal Industry of People's Republic of China (1984) Code for mining hydrogeology, Beijing 51–98

Wang Z, Li T, Chen L (2007) Determination of construction parameters for the blockage of faults by grouting. Hydrogeol Eng Geol 34(2):113–115

Wolkersdorfer C (2004) Contemporary reviews of mine water studies in Europe, part 1. Mine Water Environ 23:162–182

Yan S, Li Y (2007) The mechanism and countermeasures of water inrush caused by badly sealed drillings. Proceedings, of Annual Symp for Geological Soc of China, Coal Geology Committee of China Coal Soc, China National Coal Labor Protection Institute of Science and Technology, 2007. (8):54–56

Younger PL (2004) Mining impacts on the fresh water environment: technical and managerial guidelines for catchment scale management. Mine Water Environ (23):2–80

Yunsheng Q (2002) The application of pre-grouting in gateway intersection with fault. Express Info Min Ind (2):12–14

Zhan J (1978) The influence of non-sealed drillings to mine construction. Nonferrous Metals (Mining Section) (6):15–17

Zhang J, Tan Y (2005) The recognition and control of the inundation danger to shaft from surface water. Mod Occup Safe (10):56–57

Tan Z (1999) Preliminary analysis for groundwater inrush mechanism of fault. Min Safe Environ Prot (3):21–23

Zhong P (2007) Treatise for the stope of coal pillar with non-sealed drillings. Heilongj Land Resour (9):35